29th Congress of the International Council of the Aeronautical Sciences
St. Petersburg, Russia; September 7-12, 2014

ON THE COMPENSATION AND DAMPING OF ROLL INDUCED BY WAKE VORTICES

Campos, L.M.B.C.*, Marques, J.M.G.**
***Instituto Superior Técnico (IST)**
****Universidade Lusófona de Humanidades e Tecnologias (ULHT)**
LAETA (Associeted Laboratory for Energy, Transport and Aeronautics)
Lisboa, Portugal.

Abstract

The effect of the wake of a leading aircraft on a following aircraft is demonstrated by calculating the rolling motion consisting of three terms: (i) the free rolling motion due to initial bank angle and roll rate; (ii) the forced wake response due the rolling moment induced by the wake encounter; (iii) the forced control response due to aileron deflection to counter the wake vortex effects. It is shown that in the absence of control action, the roll rate of the following aircraft goes through a peak, and then decays, leading to a constant asymptotic bank angle; the latter is a measure of the magnitude of the wake effect, e.g. is larger for weaker damping. The exact analytical solution of the roll equation appears as a power series of a damping factor, whose coefficients are exponential integrals of time. The theory is used to simulate 15 combinations of wake vortex encounters between leading and following aircraft in the 5 ICAO/FAA weight categories: light, medium, heavy, special (B757) and very large (A380).

1 Introduction

The separation between aircraft due to wake effects determines aircraft spacing at the take-off and landing, and hence runway and airport capacity. This is the motivation for the current research on the topic [1-6]. The separation rules of ICAO and FAA are empirical, and can be compared with a formula for the separation distances [7]. The method to deduce the separation distance can also be applied to aircraft response to wake effects [8]. There is an extensive literature on wake effects [9-22] as early references. The response to wakes is affected by the application of controls and damping effects that are considered in the present paper, as an extension of an earlier analytical theory [8]. The starting point is the derivation of the rolling moment equation (section 2), whose exact analytical solution (section 3) is applied to vortex wake encounters for 15 combinations of leading and following aircraft (section 4).

The rolling moment equation (Section 2) involves the rolling moment due to the wake (sub-section 2.1) and the control moment due to aileron deflection (sub-section 2.2). Balancing the latter two specifies the aileron schedule that would exactly compensate wake induced roll effect (sub-section 2.3). Often the latter effect exceeds the available roll control power, either in terms of maximum deflection or maximum rate and in this general case the roll response of the following aircraft must be considered (Section 3). The rolling motion of the following airplane will consist of: (i) a free response to arbitrary initial condition (sub-section 3.1) as regards bank angle and roll rate; (ii) forced response to the wake encounter and aileron deflection (sub-section 3.2). Both responses will be affected by the aerodynamic damping (sub-section 3.3), especially for longer times. The application to vortex wake encounters (Section 4) starts with a detailed discussion of a particular case (sub-section 4.1), namely leading and following aircraft of the same special weight class (B757-200). Retaining the same following aircraft (B757-200) the comparison is made (sub-section 4.2) with leading aircraft of the other four categories, namely light (Jetstar),

medium (B737-200), heavy (B747-100) and very large (A380-100). Finally the same set of 5 leading aircraft of each weight class is considered for two other cases of following aircraft (sub-section 4.3), namely light and heavy.

2 Rolling moment equation for vortex encounter

2.1 Rolling moment induced by a vortex pair

The main effect of the wake of a leading aircraft on a following aircraft is to induce [7] a rolling moment:

$$R = -\frac{1}{2} C_{L_\alpha} \rho U \int_{-b/2}^{b/2} y\, c(y)\, w(y)\ dy; \tag{1}$$

the chord is a linear function of spanwise coordinate [8] for a trapezoidal wing

$$c(y) = \frac{2\bar{c}}{1+\lambda}\left[1 + \frac{(\lambda-1)}{b} 2|y|\right], \tag{2}$$

where the mean geometric chord $\bar{c}$ and taper ratio λ are specified by the root c_r and tip c_t chords:

$$2\bar{c} \equiv c_t + c_r, \qquad \lambda \equiv \frac{c_t}{c_r}. \tag{3a,b}$$

It remains to specify the downwash $w(y)$, that depends [23, 24] on the vortex model assumed. For an Hallock-Burnham (HB) vortex [25] the tangential velocity is given by:

$$w_0(r) = \frac{\Gamma_0}{2\pi} \frac{r}{r^2 + a^2}, \tag{4}$$

where the vorticity may be introduced [26] for the peak velocity at the vortex core radius:

$$\Omega a / 4 = w_{0\max} \equiv w_0(a) = \Gamma_0 / 4\pi a. \tag{5}$$

Instead of a single HB-vortex:

$$2w_0(r) = \frac{\Omega a^2 r}{r^2 + a^2}, \tag{6}$$

the wake of the leading aircraft is represented by a pair of possibly dissimilar counter-rotating HB-vortices, with vorticities $\Omega_r, -\Omega_l$, core radii a_r, a_l and axis at y_r, y_l parallel to the flight path:

$$2w(y) = \Omega_r a_r^2 \frac{y - y_r}{a_r^2 + (y - y_r)^2} - \Omega_\ell a_\ell^2 \frac{y - y_\ell}{a_\ell^2 + (y - y_\ell)^2}, \tag{7}$$

and lying at the same altitude. Substitution of (2) and (7) in (1) specifies the rolling moment for any spanwise vortex pair position, i.e. either vortex within, outside or partly inside the span of the following aircraft.

The rolling moment (1) is specified by:

$$2R = -\frac{C_{L_\alpha} \rho U \bar{c} \Omega_r a_r^2}{1+\lambda} \times \int_{-b/2}^{b/2} y\left(1 + \frac{\lambda - 1}{b} 2|y|\right) \frac{y - y_r}{a_r^2 + (y - y_r)^2} dy + \frac{C_{L_\alpha} \rho U \bar{c} \Omega_l a_l^2}{1+\lambda} \times \int_{-b/2}^{b/2} y\left(1 + \frac{\lambda - 1}{b} 2|y|\right) \frac{y - y_l}{a_l^2 + (y - y_l)^2} dy. \tag{8}$$

The rolling moment is thus given by:

$$R = -\frac{C_{L_\alpha} \rho U \bar{c} b}{1+\lambda} \left(\Omega_r a_r^2 h_r - \Omega_l a_l^2 h_l\right), \tag{9}$$

where h_r is a dimensionless encounter factor:

$$4h_r = J_{1r} + (\lambda - 1) J_{2r}, \tag{10}$$

involving the integrals:

$$J_{1r} \equiv \frac{2}{b} \int_{-b/2}^{b/2} \frac{y(y - y_r)}{a_r^2 + (y - y_r)^2} dy, \tag{11a}$$

$$J_{2r} \equiv \frac{4}{b^2} \int_{0,0}^{b/2,-b/2} \frac{y^2 (y - y_r)}{a_r^2 + (y - y_r)^2} dy, \tag{11b}$$

where the second integral is evaluated twice at each limit. Corresponding formulas apply to h_l, and a similar change of variable, allows elementary evaluation [23] of the integrals:

$$u \equiv (y - y_r)/a_r: \quad J_{1r} = \frac{2}{b} \int_{-(b/2+y_r)/a_r}^{(b/2-y_r)/a_r} \frac{u(y_r + a_r u)}{1+u^2} du =$$

$$\left[\frac{y_r}{b} \log(1+u^2) + 2\frac{a_r}{b}(u - \arctan u)\right]_{-(b/2+y_r)/a_r}^{(b/2-y_r)/a_r}$$

$$J_{2r} = \frac{4}{b^2} \times$$

$$\int_{-y_r/a_r,-y_r/a_r}^{(b/2-y_r)/a_r,-(b/2+y_r)/a_r} \frac{y_r^2 u + 2 y_r a_r u^2 + a_r^2 u^3}{1+u^2}\, du =$$

$$= 2\left[\left(\frac{y_r^2 - a_r^2}{b^2} \right) \log\left(1+u^2\right) + \right.$$

$$\left. +4\frac{a_r y_r}{b^2}\left(u - \arctan u\right) + \frac{a_r^2}{b^2} u^2 \right]_{-y_r/a_r,-y_r/a_r}^{(b/2-y_r)/a_r,-(b/2+y_r)/a_r}$$

(12a,b)

Substitution of (12a,b) in (10) and (9) completes the evaluation of rolling moment, for dissimilar vortices and zero bank angle. The opposite case of similar vortices and non-zero bank angle has been considered elsewhere [27]. The bank angle correction becomes important if the aircraft rolls significantly as a consequence of the wake encounter.

2.2 Roll equation with damping and controls

For substitution in the roll dynamics equation, including the effects of aerodynamic damping and flight controls, the rolling moment induced by the pair of dissimilar HB-vortices is used in the form (9), where the dimensionless encounter factors h_r, h_l, (10) are specified by (12a,b), viz.:

$$4h_r = 2 + \left(y_r/b\right) h_{1r} - 2\left(a_r/b\right) h_{2r} + \left(\lambda - 1\right)$$

$$\left\{ 1 + 2\left[\left(y_r^2 - a_r^2\right)/b^2 \right] h_{4r} - 8\left(a_r y_r/b^2\right) h_{3r} \right\}, \quad (13)$$

where:

$$h_{1r} = \log\left\{ \left[(b/2 - y_r)^2 + a_r^2 \right] / \left[(b/2 + y_r)^2 + a_r^2 \right] \right\}$$

$$h_{2r} = \arctan\left[(b/2 + y_r)/a_r \right] + \arctan\left[(b/2 - y_r)/a_r \right]$$

$$h_{3r} = 2\arctan\left(y_r/a_r\right) +$$

$$+ \arctan\left((b/2 - y_r)/a_r \right) - \arctan\left((b/2 + y_r)/a_r \right)$$

$$h_{4r} = \log\left\{ \left[\left(a_r^2 + b^2/4 + y_r^2\right)^2 - b^2 y_r^2 \right] / \left(a_r^2 + y_r^2\right)^2 \right\}$$

(14a-d)

Note that the last three terms on the r.h.s. of (13) vanish for a rectangular wing $\lambda = 1$. The average dimensionless encounter factor h is defined by:

$$\Omega_r a_r^2 h_r - \Omega_l a_l^2 h_l \equiv \left(\Omega_r - \Omega_l\right) a^2 h, \quad (15)$$

where a is taken to be the mean vortex radius:

$$a \equiv \left(a_r + a_l\right)/2. \quad (16)$$

The simplest case is that of vortices with equal radii $a_r = a_l = a$, symmetrically placed $y_r = -y_l = y_0$ when $h_r = h_l = h$; in general $h_r \neq h_l$, for a asymmetrically placed vortices $y_r \neq -y_l$ with distinct vortex radii $a_r \neq a_l$, and the average encounter factor is defined by (15). Substitution of (15) specifies (9) the rolling moment:

$$R = -\frac{2C_{L_\alpha} \rho U_2 S_2}{1+\lambda} a^2 h\, \Omega(t), \quad (17)$$

whose time dependence is specified by that of the sum of the vorticities of the right and left vortices:

$$2\Omega(t) \equiv \Omega_r(t) - \Omega_l(t). \quad (18)$$

These time dependences are similar [7] for identical vortex radii:

$$a_l = a_r \equiv a: \qquad \Omega(t) = \frac{\Gamma_0}{2\pi\eta t} \exp\left(-\frac{a^2}{2\eta t} \right), \quad (19)$$

where the wake vortex circulation strength [24, 25] is specified by:

$$\Gamma_0 = \frac{c_{r_1} W_1}{\rho U_1 S_1}, \quad (20)$$

and the index "1" applies to the leading aircraft. Substitution of (20) into (19) specifies the time dependence (17) of the induced rolling moment:

$$R = -\frac{2h}{1+\lambda} \frac{C_{L_\alpha}}{2\pi} W_1 \frac{U_2}{U_1} \frac{S_2}{S_1} c_{r_1} \frac{a^2}{\eta t} \exp\left(-\frac{a^2}{2\eta t} \right), \quad (21)$$

which appears in the roll dynamics equation, with one degree-of-freedom, i.e. no coupling to other axis:

$$I_2 \ddot{\varphi} - \frac{1}{2} \rho U_2 S_2 \left(b_2\right)^2 C_{\dot{\varphi}} \dot{\varphi} =$$

$$\rho S_2 b_2 \left(U_2\right)^2 C_\delta \delta(t) \quad . \quad (22)$$

$$- \frac{2h}{1+\lambda} \frac{C_{L_\alpha}}{2\pi} W_1 \frac{U_2}{U_1} \frac{S_2}{S_1} c_{r_1} \frac{a^2}{\eta t} \exp\left(-\frac{a^2}{2\eta t} \right)$$

Writing the roll moment of inertia in terms of mass and radius of gyration:

$$I_2 = m(r_2)^2 = W_2 (r_2)^2 / g \,, \tag{23}$$

leads to the roll dynamics equation in the form:

$$\ddot{\varphi} - \frac{1}{2} \frac{\rho U_2 S_2}{W_2 / g} \left(\frac{b_2}{r_2} \right)^2 C_{\dot{\varphi}} \dot{\varphi} = \frac{\rho S_2 b_2}{W_2 / g} \left(\frac{U_2}{r_2} \right)^2 C_\delta \delta(t) \,,$$
$$- \frac{2h}{1+\lambda} \frac{C_{L_\alpha}}{2\pi} \frac{W_1}{W_2} \frac{S_2}{S_1} \frac{U_2}{U_1} \left(\frac{a}{r_2} \right)^2 \frac{c_{r_1} g}{\eta t} \exp\left(- \frac{a^2}{2\eta t} \right) \tag{24}$$

which will be used in the sequel.

2.3 Aileron schedule to compensate for a vortex encounter

The simplest result to follow from (24) is that there will be no roll motion, i.e. the wake vortex encounter will be compensated by the aileron deflection as a function of time specified by:

$$\delta(t) = \frac{1}{C_\delta} \frac{2h}{1+\lambda} \frac{C_{L_\alpha}}{2\pi} \frac{W}{\rho S_1 U_1 U_2} \frac{c_{r_1}}{b_2} \frac{a^2}{\eta t} \exp\left(- \frac{a^2}{2\eta t} \right) . \tag{25}$$

The last exponential factor in (25), is the same as in the vorticity (19, 20), and shows that its peak occurs at the time:

$$t_* = a^2 / 2\eta, \; \Omega_{\max} = \Omega(t_*) = \frac{\Gamma_0}{\pi a^2 e} = \frac{c_{r_1} W_1}{e \pi \rho U_1 S_1 a^2} \,, \tag{26a,b}$$

and the corresponding aileron deflection would occur at the same time:

$$\delta_* \equiv \delta(t_*) = \frac{1}{C_\delta} \frac{2}{e} \frac{h}{1+\lambda} \frac{C_{L_\alpha}}{2\pi} \frac{W}{\rho S_1 U_1 U_2} \frac{c_{r_1}}{b_2} \,. \tag{26c}$$

As an example, the case of two Boeing 757-200 flying one behind the other is considered. The data needed to calculate the maximum aileron deflection is given in *Table I*, with basic data from open sources [29, 30] at the top, and at the bottom, data derived by calculation using the formulas in this paper. The vortex core radius was taken to be 3% of the wing span. For identical vortices with axis at mid-span $y_r = y_\ell = b/2$, the encounter factor (13; 14a-d) is given by:

$$h_1 = \log\left(1 + b^2 / a^2\right), \quad h_2 = \arctan\left(b/a\right), \tag{27a,b}$$

$$h_3 = \arctan\left[b/(2a) \right] - \arctan\left(b/a\right), \tag{27c}$$

$$h_4 = \log\left[\frac{1 + b^2/a^2}{\left(1 + b^2/4a^2\right)^2} \right], \tag{27d}$$

$$h = \frac{1}{2} + \frac{1}{8} h_1 - \frac{a}{2b} h_2 + - \frac{a}{b} h_3$$
$$+ (\lambda - 1) \left[\frac{1}{4} + \frac{1}{2} \left(\frac{1}{4} - \frac{a^2}{b^2} \right) h_4 \right] . \tag{27e}$$

Using the lift slope $C_{L_\alpha} = 2\pi$ for a Joukowski airfoil, from (26c) follows the aileron deflection $\delta_* = 17.26^\circ$ that compensates the induced rolling moment at the induced rolling moment at the peak vorticity. If the maximum aileron deflection is (28a) then the ratio (28b):

$$\delta_{\max} = 15^\circ : \qquad 0.869 = \frac{\delta_*}{\delta_{\max}} = \frac{\Omega}{\Omega_{\max}} = \psi \,, \tag{28}$$

specifies the fraction of the maximum vorticity that the roll control power available is able to compensate. If $\psi < 1$ the following aircraft must move further behind the leading aircraft to a safe separation distance (SSD) for which [7] it has sufficient roll control power to compensate for the wave vortex.

3 Combination of free, forced and airleron control responses

3.1 Free response and aileron deflection

The preceding case (Section 4) of an aileron control law which compensates the wake vortex encounter is the only situation in which there is no aircraft roll response, because the forced response to the ailerons (ii) exactly balances the response to the wake vortex (iii), leaving only the free response (i), which is zero if there are no initial perturbation. The three terms of the response (i,ii,iii) are calculated next in turn, starting with the free response $\phi_f(t)$, which is the solution of the roll equation (24) without forcing terms on the r.h.s., viz.:

$$\ddot{\phi}_f + \bar{\mu} \dot{\phi}_f = 0 \,, \tag{29}$$

where the overall damping coefficient is specified by:

$$\bar{\mu} \equiv -\frac{1}{2}\frac{\rho U_2 S_2}{W_2/g}\left(\frac{b_2}{r_2}\right)^2 C_{\dot{\phi}}, \qquad (30)$$

and the damping time by $1/\bar{\mu}$.

The solution of (29) is the free response:

$$\phi_f(t) = A + Be^{-\bar{\mu}t}, \qquad (31)$$

where the constants of integration A, B are determined from the initial bank angle ϕ_0 and roll rate $\dot{\phi}_0$ at time zero:

$$\phi_0 \equiv \phi_f(0) = A + B, \quad \dot{\phi}_0 = \dot{\phi}_f(0) = -\bar{\mu}B. \qquad (32)$$

It follows that the free response (31) is given by:

$$\phi_f(t) = \phi_0 + \left(\dot{\phi}_0/\bar{\mu}\right)\left[1 - e^{-\bar{\mu}t}\right], \qquad (33)$$

for arbitrary initial bank angle ϕ_0 and roll rate $\dot{\phi}_0$. The forced response to the ailerons $\phi_c(t)$ is even simpler, since it is a particular solution of the roll dynamics equation (24), omitting the last term on the r.h.s. side representing wake vortex effects:

$$\ddot{\phi}_c + \bar{\mu}\dot{\phi}_c = \nu, \qquad (34)$$

where the aileron deflection was taken to be maximum in the aileron control parameter:

$$\nu \equiv \frac{\rho S_2 b_2}{W_2/g}\left(\frac{U_2}{r_2}\right)^2 C_\delta \delta_{\max}. \qquad (35)$$

The forced response to constant aileron deflection is a bank angle varying linearly with time:

$$\phi_c(t) = \frac{\nu}{\bar{\mu}}t \equiv 2\frac{U_2}{b_2}\frac{C_\delta}{C_{\dot{\phi}}}\delta_{\max} t, \qquad (36)$$

showing that in the presence of damping the roll rate is constant $\dot{\phi}_c(t) = \nu/\bar{\mu}$. Note that in the absence of damping:

$$\mu = 0: \qquad \ddot{\phi}_c = \nu, \qquad (37)$$

the roll acceleration would be constant, and hence the roll rate would be linear function of time (38a):

$$\dot{\phi}_c(t) = \nu t, \qquad \phi_c(t) = \frac{1}{2}\nu t^2, \qquad (38a,b)$$

and the bank angle a quadratic function of time (38b).

3.3 Response forced by wake encounter

The response to the wake encounter would be almost as simple as for constant aileron deflection (subsection 3.1) if the induced rolling moment is taken to be constant [28]. Taking into account the dependence of the induced rolling moment on time leads to a less simple response $\phi_w(t)$, specified by a particular integral of the roll dynamics equation (24), without the first term on the r.h.s.:

$$\ddot{\phi}_w + \bar{\mu}\dot{\phi}_w = -\bar{\xi}t^{-1}\exp\left(-a^2/2\eta t\right), \qquad (39)$$

where the vortex wake effect is specified by:

$$\bar{\xi} \equiv \frac{2h}{1+\lambda}\frac{C_{L_\alpha}}{2\pi}\frac{W_1/S_1}{W_2/S_2}\frac{U_2}{U_1}\left(\frac{a}{r_2}\right)^2\frac{c_{r_1}g}{\eta}. \qquad (40)$$

It is convenient to introduce a dimensionless time divided by the time (26a) of peak vorticity:

$$\tau \equiv t/t_* = 2\eta t/a^2, \qquad \Phi(\tau) = \phi_w(t), \qquad (41a,b)$$

so that the roll response forced by the wake vortex satisfies:

$$\ddot{\Phi} + \mu\dot{\Phi} = -\left(\xi/\tau\right)e^{-1/\tau}, \qquad (42)$$

where the dimensionless aerodynamic damping (30) and vortex effect (40) are given respectively by:

$$\mu \equiv \frac{\bar{\mu}a^2}{2\eta} = -\frac{1}{4}\left(\frac{b_2}{r_2}\right)^2\frac{\rho S_2 a}{W_2/g}\frac{U_2 a}{\eta}C_{\dot{\phi}}, \qquad (43a)$$

$$\xi \equiv \frac{\bar{\xi}a^2}{2\eta} = \frac{2h}{1+\lambda}\frac{C_{L_\alpha}}{2\pi}\frac{W_1/S_1}{W_2/S_2}\frac{U_2}{U_1}\left(\frac{a}{r_2}\right)^2\frac{c_{r_1}a^2 g}{2\eta^2} \qquad (43b)$$

The forced solution of (42) is sought by the method of variation of parameters, i.e. as the free solution (31) with non-constant coefficients:

$$\Phi(\tau) = A(\tau) + B(\tau)e^{-\mu\tau}, \qquad (44)$$

that can be chosen at will.

Substitution of (44) into (42) yields:

$$-\left(\xi/\tau\right)e^{-1/\tau} = \left(\ddot{A} + \mu\dot{A}\right) + \left(\ddot{B} - \mu\dot{B}\right)e^{-\mu\tau}, \qquad (45)$$

that is satisfied in particular by:

$$A(\tau) = 0, \quad \dot{B} - \mu B = -\xi\int \tau^{-1}e^{-1/\tau}e^{\mu\tau}d\tau, \qquad (46a,b)$$

viz. the first arbitrary function is not needed (46a), and the second satisfies a first-order differential equation (46b), for which a particular solution is obtained again by the method of variation of parameters:

$$B(\tau) = D(\tau) e^{\mu\tau}; \quad (47a)$$

substitution of (47a) in (46b) specifies the function $D(\tau)$ by:

$$-\xi \int \tau^{-1} e^{-1/\tau} e^{\mu\tau} d\tau = \dot{B} - \mu B = \dot{D} e^{\mu\tau}. \quad (47b)$$

Integration of (47b) and substitution in (47a), leads together with (46a) to (44) the forced response:

$$\Phi(\tau) = D(\tau) = -\xi \int e^{-\mu\tau} d\tau \int \tau^{-1} e^{-1/\tau} e^{\mu\tau} d\tau, \quad (48)$$

to the wake vortex.

3.3 Time evolution of the forced response

The total roll response is the sum of the free response (33) with the forced responses to the ailerons (36) and the wake vortex (41b):

$$\phi(t) = \phi_f(t) + \phi_c(t) + \phi_w(t). \quad (49)$$

Assuming that the initial bank angle and the roll rate are zero there is no free response $\phi_1(t) = 0$ in (33), and the total forced response

$$\phi_0 = 0 = \dot{\phi}_0: \quad \phi(t) = \phi_c(t) + \Phi\left(2\eta t / a^2\right), \quad (50)$$

consists of: (i) the response to the ailerons, given explicitly by (36) in the presence of damping , and by (38b) in the absence of damping; (ii) the response to the wake vortex, that in the presence of damping is given by (48). In the absence of damping the exponential integral [29]:

$$T = 1/\tau: \; E_0(T) \equiv \int_T^\infty T^{-1} e^{-T} dT = \int_0^{1/\tau} \tau^{-1} e^{-1/\tau} d\tau = E_0(1/\tau), \quad (51)$$

appears in (48) with $\mu = 0$:

$$\mu = 0: \Phi_0(\tau) = -\xi \int E_0(1/\tau) \, d\tau, \quad (52)$$

in agreement with[8]. This earlier result is generalized next to include the effects of damping.

Since the dimensionless roll rate in the absence of damping (52) is specified by an exponential integral of order zero:

$$-\xi^{-1} \dot{\Phi}_0(\tau) = E_0(1/\tau) = \int \tau^{-1} e^{-1/\tau} d\tau, \quad (53)$$

the comparison with the dimensionless roll rate in the presence of damping (48)

$$-\xi^{-1} \dot{\Phi}(\tau) = e^{-\mu\tau} \int \tau^{-1} e^{-1/\tau} e^{\mu\tau} d\tau, \quad (54)$$

suggests considering the damping integral:

$$H \equiv -\left[e^{\mu\tau} \dot{\Phi}(\tau) - \dot{\Phi}_0(\tau)\right] / \xi = \int \tau^{-1} e^{-1/\tau} \left(e^{\mu\tau} - 1\right) d\tau \quad (55)$$

.

Expanding the exponential in power series leads to:

$$H = \sum_{n=1}^\infty \frac{\mu^n}{n!} \int e^{-1/\tau} \tau^{n-1} d\tau, \quad (56)$$

where the coefficients are exponential integrals of order n:

$$T = 1/\tau: \; \int_0^{1/\tau} e^{-1/\tau} \tau^{n-1} d\tau = E_n(1/\tau), \quad (57)$$

and thus:

$$H = \sum_{n=1}^\infty \frac{\mu^n}{n!} E_n(1/\tau). \quad (58)$$

Substituting (58) and (53) in (55) yields:

$$\dot{\Phi}(\tau) = -\xi e^{-\mu\tau} \left\{ E_0(1/\tau) + \sum_{n=1}^\infty \frac{\mu^n}{n!} E_n(1/\tau) \right\}, \quad (59)$$

that specifies the dimensionless roll response:

$$\Phi(\tau) = -\xi \sum_{n=0}^\infty \frac{\mu^n}{n!} \int e^{-\mu\tau} E_n(1/\tau) \, d\tau, \quad (60)$$

as a series of powers of the damping, with exponential integrals of order n as coefficients. If the damping is weak, only the first terms of the series are needed, e.g. the first two for $\mu^2 << 1$.

4 Wake vortex encounters for combinations of 5 classes of aircraft

The roll response to wake vortex encounters will be considered for 15 combinations of leading and following aircraft, presenting only the main result, namely the bank angle and roll rate as a function of time. The following aircraft is of the special class (B757-200) for which data appears in the Table I is retained. The leading aircraft is replaced by alternatives from the other four weights classes, namely: (i) a medium (B737-200) and a very large (A380-100) following aircraft (data from [29, 30]); (ii) a light (Lockheed Jetstar) and a heavy (B747-

100) leading or following aircraft (data from [31]); The Figure 1 shows the roll rate (top) and bank angle (bottom) as a function of the time for the same special (s) following aircraft, comparing the five classes of leading aircraft, namely light (l), medium (m), special (s), heavy (h) and very large (v). Apart from differences of scale the Figure 1 coincides with the Figure 3 for the same special (s) leading and following aircraft (s-s). Replacing the leading special aircraft (s-s) by a medium (m-s) or light (l) aircraft leads to a smaller peak roll rate at an earlier time (Figure 1 top) and a smaller ultimate bank angle also at an earlier time (Figure 1 bottom). Conversely replacing the leading special aircraft (s-s) by a heavy (h-s) or a very large (v-s) aircraft leads to a larger roll rate (Figure 1 top), and larger ultimate bank angle (Figure 1 bottom), in both cases at a later time. The peak roll rate $\dot{\phi}_{\max}$ and time $t_{\max}$ for which it occurs, and asymptotic bank angle $\phi_{\max}$ and time t_{∞} to which 1% of $\phi_{\max}$ are indicated in Table 1 for the five combinations of special following aircraft (… - s) and leading light (l-s), medium (m-s), special (s-s), heavy (h-s) and very large (v-s) aircraft.

The same 5 classes of leading aircraft considered in the Figure 1 for their wake vortex effects on a special (s) following aircraft, are reconsidered for a heavy (h) and for a light (l) following aircraft respectively in the figures 2 and 3. The Figure 2 shows that a heavy following aircraft is much less affected than the special following aircraft in the Figure 1 by the wake vortices of the same leading aircraft: (i) lower peak roll rate reached sooner (Figure 2, top); (ii) smaller asymptotic bank angle also reached sooner (Figure 2, bottom). The differences (i) and (ii) are quantified in Table 1 for special following aircraft, in the Table 2 for heavy aircraft and in the Table 3 for light following aircraft. The Table 3 corresponds to the Figure 3 for the light following aircraft, that is the most susceptible to wake effects regarding roll rate (Figure 3, top) and bank angle (Figure 3, bottom). Large roll rates leading large asymptotic bank angles with a long time delay, imply that the following aircraft would roll several times before the aerodynamic damping would overcome the roll disturbance caused on the following aircraft by the wake vortex of the leading aircraft. Roll rates above 9º/s and asymptotic bank angle of more than 90º more than one minute later, as seen in the Table 3 for a light behind a very large or heavy aircraft, indicate an insufficient roll control power to cope with wake vortex effects. In such cases safe flight requires a much increased separation.

5 Discussion

The effect of damping and controls on an aircraft wake encounter has been modeled using the following assumptions: (i) the wake of the leading aircraft is represented by a pair of counterotating Hallock-Burnham vortices, with arbitrary circulations and core radii; (ii) the vorticity decays with distance due to a turbulent kinematic viscosity, according to a law which is consistent with flight data from the Memphis data base; (iii) the rolling moment induced in the following aircraft is calculated assuming it flies aligned behind the leading aircraft; (iv) the rolling moment equation is solved analytically including the effect of the control surface deflection (e.g. ailerons) and of aerodynamic damping; (v) the airplane response, in terms of roll rate and bank angle as a function of time is discussed in detail for identical leading and following special (s) aircraft; (vi) this is then extended to all classes of leading aircraft, by adding light (l), medium (m), heavy (h) and very large (v); (vii) to the preceding five wake vortex encounters (v-vi) are added 10 more retaining the same five leading aircraft (l, m, s, h, v) and replacing the special (s) following aircraft by light (l) and heavy (h).

The vorticity behind the leading aircraft increases as the wing tip vortices roll-up, and ultimately must decay due to the atmospheric turbulent kinematic viscosity, so that it goes through a peak in between. A similar variation applies to the rolling moment induced on the following aircraft, leading to a roll rate ultimately decays due to aerodynamic roll damping. Thus the bank angle increases until it approaches a constant asymptotic value. Considering five classes of aircraft, namely light, medium, special, heavy and very large,

depending on which is leading and which is following, there are considerable differences in: (i) the peak roll rate and time when it occurs; (ii) the asymptotic bank angle and the time taken to come within 1% of the final value. These differences have been quantified in tables and illustrated by plots of roll rate and bank angle as a function of time. The numerical results are based on a theoretical model of wake vortex response that is explicit on the dependences on aircraft, flight and atmospheric parameters.

6 Acknowledgements

This work was started under the S-Wake project of EC Aeronautics Programme and has benefited from comments of other partners in this activity.

7 References

[1] SHEN, S., DING, F., HAN, J., LIN, Y-L., ARYA, S.P. and PROCTOR, F. H. Numerical modeling studies of wake vortices: real case simulations, 1999, AIAA Paper 99-0755, 37th Aerospace Sciences Meeting, Reno, Nevada.

[2] VICTROY, D. and NGUYEN, T. A numerical simulation study to develop an acceptable wake encounter boundary for a B737-100 airplane, 1993, AIAA paper.

[3] PERRY, R.R., HINTON, D.A. and STUEVER, R.A. NASA wake vortex research for aircraft spacing, 1996, AIAA paper.

[4] HINTON, D.A. An Aircraft Vortex Spacing System (AVOSS) for dynamical wake vortex spacing criteria, 1996, 78th Fluid Mechanics Panel & Symposium on the Characterization and modification of wakes from lifting vehicles in fluids, Trondheim, Norway.

[5] HINTON, D.A., CHARNOCK, J.K., BAGWELL, D.R. and GRIGSBY, D. NASA Aircraft Vortex Spacing System Development Status, 1999, AIAA 37th Aerospace Sciences Meeting, Reno, Nevada.

[6] JACKSON, W. (Ed) Wake Vortex Prediction: An Overview, Appendix F: Hazard Definition, 2001, Transportation Department of Canada TP 13629E.

[7] CAMPOS, L.M.B.C. and MARQUES, J.M.G. On Runway Capacity and Wake Vortex Safe Separation Distance (SSD), 2013, in Proceedings of the Third SESAR Innovation Days, Stockholm, Eurocontrol/SESAR-JU.

[8] CAMPOS, L.M.B.C. and MARQUES, J.M.G. On wake vortex response for all combinations of five classes of aircraft, *The Aeronautical Journal*, 2004, Paper 2718, June, pp. 295-310.

[9] MCGOWAN, W.A. Calculated Normal Load Factors on Light Airplanes Traversing the Trailing Vortices of Heavy Transport Airplanes, 1961, NASA TN D-829.

[10] IVERSEN, J.D. and BERNSTEIN, S. Trailing Vortex Effects on Following Aircraft, *J Aircr*, 1974, 11, (1), pp. 60-61.

[11] NELSON, R. C. The Dynamic Response of Aircraft Encountering Aircraft Wake Turbulence, 1974, Tech. Report AFFDL-TR-74-29, Air Force Flight Dynamics Laboratory, Wright-Patterson Air Force Base, Ohio.

[12] SAMMONDS, R. I. and STINNETT, G. W. Hazard Criteria for Wake Vortex Encounters, 1975, NASA TM X-62,473.

[13] SAMMONDS, R. I., STINNETT, G. W. and LARSEN, W.E. Wake Vortex Encounter Hazard Criteria for Two Aircraft Classes, 1976, NASA TM X-73,113.

[14] NELSON, R.C. Dynamic Behaviour of an Aircraft Encountering Wake Turbulence, *J Aircr*, 1976, 13, (9), pp. 704-708.

[15] MCWILLIAMS, I. G. Hazard Extent About Aircraft Trailing Wake Vortices-Analytic Approach, 1977, Proceedings of the Aircraft Wake Vortices, Conference, edited by J. N. Hallock, Report No. FAA-RD-77-68, U. S. Dept. of Transportation, pp. 23-30.

[16] TINLING B. E. Estimation of Vortex-Induced Roll Excursions Based on Flight and Simulation Results, 1977, Proceedings of the Aircraft Wake Vortices Conference, edited by J. N. Hallock, Report No. FAA-RD-77-68, U. S. Dept. of Transportation, March 15-17, pp 11-22.

[17] TINLING B. E. Estimates of the Effectiveness of Automatic Control in Alleviating Wake Vortex Induced Roll Excursions, 1977, NASA TM-73,267.

[18] MCMILLAN, O.J. NIELSEN, J.N. SCHWIND, R. G. and DILLENIUS, M. F. E. Rolling Moments in a Trailing-Vortex Flow Field, *J Aircr*, 1978, 15, (5), pp. 280-286.

[19] ROSSOW, V. J. AND TINLING B. E. Research on Aircraft/Vortex-Wake Interactions to Determine Acceptable Level of Wake Intensity, *J Aircr*, 1988, 25, (4), pp. 481-492.

[20] STUEVER, R. A. and GREENE, G. C. An analysis of wake-vortex hazards for typical transport aircraft, 1994, AIAA Paper 94-0810.

[21] HINTON, D.A. and TATNALL, C.R. A candidate wake vortex strength definition for application to the NASA aircraft vortex space system (AVOSS), 1997, NASA Tech. Memo TM-110343.

[22] BELOTSERKOVSKY, A. Hazard Definition, Appendix F, in Wake vortex prediction: an overview, 2001, W. Jackson (Ed), Dept. Transp. Canada TP13629.

[23] MILNE-THOMSON, L.N. Theoretical aerodynamics, 1958, Dover.
[24] CAMPOS, L. M. B. C. Complex analysis with applications to flows and fields, 2011, CRC Press.
[25] HALLOCK, J. N. and BURNHAM D. C. Decay characteristics of wake vortex from jet transport aircraft, 1997, AIAA paper 97-0060, 35th Aerosp. Sci. Meet. Exhib. 9-10 Jan., Reno, NV.
[26] CAMPOS, L. M. B. C. Transcendental representations with applications to solids and fluids, 2012, CRC Press.
[27] TATNALL, C.R. A Proposed Methodology for Determining Wake-Vortex Imposed Aircraft Separation Constraints, 1995, MSc thesis submitted at George Washington University.
[28] ABRAMOWITZ, M. and STEGUN, I. *Tables of Mathematical Functions*, 1965, Dover, New York.
[29] JACKSON, P. (Ed) *Jane's All-the-World's Aircraft 2006-2007*, 2006, MacDonald and Jane's, London.
[30] STUERVER, R.A. Airplane data base for wake-vortex hazard definition and assessment, 1995, Version 2.0, NASA Langley Research Center.
[31] HEFFLEY, R. K. and JEWELL, W. F. Aircraft handling qualities data, 1972, NASA CR- 2144.

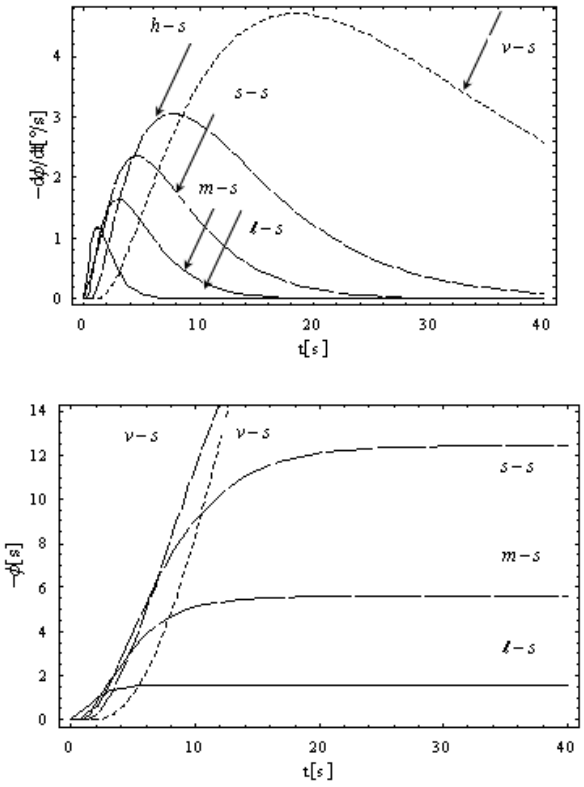

Fig. 1 – Roll rate (top) and bank angle (bottom) as a function of time for special(s) following aircraft (B757-200) comparing identical (s) and different leading aircraft, namely light (l), medium (m), heavy (h) and very large (v).

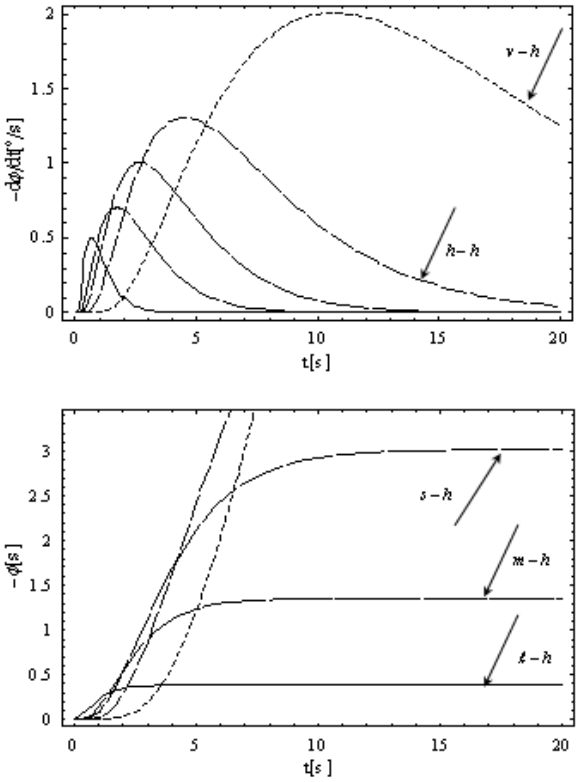

Fig. 2 – As figure 1 for light heavy following aircraft.

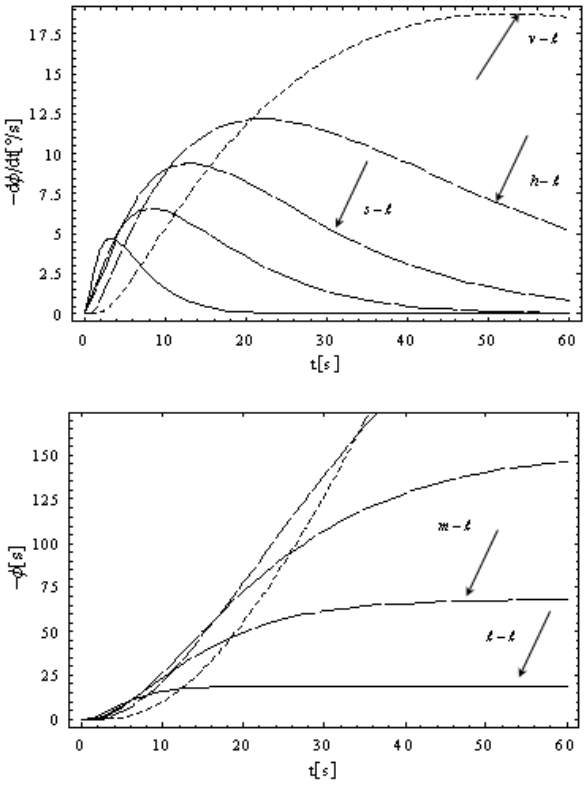

Fig. 3 – As figure 1 for following aircraft light

Table 1 – Wake vortex effects on following special aircraft.

Aircraft		Roll rate		Bank angle	
1	2	Peak value (º/s)	Peak time (s)	Asymptotic (º)	Peak time (s)
special (s)	l	1.17	1.15	1.55	6.05
	m	1.64	2.94	5.37	15.5
	s	2.35	4.60	12.4	24.2
	h	3.05	7.77	27.3	40.6
	v	4.70	18.4	99.4	96.7

Table 2 – Wake vortex effects on following heavy aircraft.

Aircraft		Roll rate		Bank angle	
1	2	Peak value (º/s)	Peak time (s)	Asymptotic (º)	Peak time (s)
heavy (h)	l	0.50	3.26	0.37	7.39
	m	0.64	8.36	1.35	7.88
	s	1.01	13.0	3.02	12.3
	h	1.31	22.0	6.64	20.8
	v	2.01	52.2	24.2	49.3

Table 3 – Wake vortex effects on following light aircraft.

Aircraft		Roll rate		Bank angle	
1	2	Peak value (º/s)	Peak time (s)	Asymptotic (º)	Peak time (s)
light (l)	l	4.69	3.27	19.06	19.75
	m	6.56	8.37	68.30	50.57
	s	9.38	13.1	152.45	79.01
	h	12.2	22.1	334.92	133.53
	v	18.8	52.3	1219.56	316.05

8 Contact Author Email Address

LMBC Campos: luis.campos@ist.utl.pt

Copyright Statement